Original Article

# Ameliorating lipopolysaccharide induced acute lung injury with Lianhua Qingke: focus on pulmonary endothelial barrier protection

**Yan Ma[1], Yunlong Hou[2,3], Yu Han[4], Yi Liu[5], Ningxin Han[5], Yujie Yin[2,3], Xiaoqi Wang[2,3], Peipei Jin[1], Zhuo He[1], Jiemeng Sun[1], Yuanjie Hao[2,3], Jing Guo[1], Tongxing Wang[2,3], Wei Feng[2,3], Hui Qi[2,3], Zhenhua Jia[1,2,3,6]**

[1]Graduate School, Hebei University of Chinese Medicine, Shijiazhuang, China; [2]Hebei Academy of Integrated Traditional Chinese and Western Medicine, Shijiazhuang, China; [3]State Key Laboratory for Innovation and Transformation of Luobing Theory, Shijiazhuang, China; [4]Department of Pharmacy, Hebei Children's Hospital, Shijiazhuang, China; [5]Graduate School, Hebei Medical University, Shijiazhuang, China; [6]Department of Respiratory, Affiliated Yiling Hospital of Hebei Medical University, Shijiazhuang, China

*Contributions:* (I) Conception and design: Z Jia, H Qi, Y Hou, Y Yin; (II) Administrative support: Z Jia, H Qi, Y Hou; (III) Provision of study materials or patients: Z Jia; (IV) Collection and assembly of data: Y Ma; (V) Data analysis and interpretation: Y Ma; (VI) Manuscript writing: All authors; (VII) Final approval of manuscript: All authors.

*Correspondence to:* Zhenhua Jia, PhD. Department of Respiratory, Affiliated Yiling Hospital of Hebei Medical University, No. 385 Xinshi North Road, Shijiazhuang 050091, China; Graduate School, Hebei University of Chinese Medicine, Shijiazhuang, China; Hebei Academy of Integrated Traditional Chinese and Western Medicine, Shijiazhuang, China; State Key Laboratory for Innovation and Transformation of Luobing Theory, Shijiazhuang, China. Email: jzhjiazhenhua@163.com; Hui Qi, PhD. Hebei Academy of Integrated Traditional Chinese and Western Medicine, No. 238 Tianshan Street, High Tech Zone, Shijiazhuang 050035, China; State Key Laboratory for Innovation and Transformation of Luobing Theory, Shijiazhuang, China. Email: qihui_qh@163.com.

**Background:** Acute lung injury (ALI)/acute respiratory distress syndrome (ARDS) has long posed challenges in clinical practice, lacking established preventive and therapeutic approaches. Lianhua Qingke (LHQK), a patented traditional Chinese medicine (TCM), has been found to have anti-inflammatory effects for ameliorating ALI/ARDS induced by lipopolysaccharide (LPS). This study aimed to investigate the effects and potential mechanisms of LHQK on endothelial protection in LPS-induced ALI/ARDS *in vivo* and in LPS-induced human pulmonary microvascular endothelial cells (HPMECs) injury *in vitro.*

**Methods:** In the animal experiment, we induced an ALI/ARDS model by intratracheal injection of LPS (5 mg/mL). LHQK (3.7 g/kg/d for low dose and 7.4 g/kg/d for high dose) or dexamethasone (DEX) (5 mg/kg/d) was administered to mice 3 days prior to LPS treatment. In the *in vitro* experiments, HPMECs were pretreated with LHQK at concentrations of 125 and 250 μg/mL for 2 hours before being stimulated with LPS (10 μg/mL). We employed lung function test, measurement of lung index, hematoxylin and eosin (H&E) staining, bronchoalveolar lavage fluid (BALF) cell counts, and inflammatory cytokine levels to assess the therapeutic effect of LHQK. Additionally, the extravasation assay of fluorescein isothiocyanate-dextran (FITC-dextran) dye and the transmembrane electrical resistance (TEER) assay were used to evaluate endothelial barrier. Barrier integrity and relevant protein validation were assessed using immunofluorescence (IF) and Western blot analyses. Furthermore, network pharmacology analysis and cellular level screening were employed to predict and screen the active ingredients of LHQK.

**Results:** Compared to the LPS group, LHQK significantly improved lung function, mitigated lung pathological injuries, reduced inflammatory cells and inflammatory cytokines [tumor necrosis factor (TNF)-α, interleukin (IL)-1β, and IL-6] levels in BALF, and inhibited the expression of vascular cell adhesion molecule-1 (VCAM-1), attenuated LPS-induced pulmonary oedema and FITC-dextran permeability, and enhanced the expression of vascular endothelial-cadherin (VE-cadherin) and occludin. *In vitro*, LHQK attenuated LPS-induced HPMECs injury by elevating TEER values and enhancing VE-cadherin and occludin protein levels. Finally, network pharmacology analysis and cellular level validation identified potential active ingredients of LHQK.

**Conclusions:** In summary, LHQK can mitigate LPS-induced inflammatory infiltration, pulmonary edema,

and pulmonary vascular endothelial barrier dysfunction in the context of ALI/ARDS. This is achieved by decreasing the levels of VCAM-1, and increasing the expression levels of barrier-associated junctions, such as VE-cadherin and occludin. Consequently, LHQK exhibits promising therapeutic potential in preventing the progression of ALI/ARDS.

**Keywords:** Lianhua Qingke (LHQK); acute lung injury (ALI); lipopolysaccharides (LPS); inflammation; endothelial barrier

Submitted Apr 29, 2024. Accepted for publication Aug 16, 2024. Published online Oct 29, 2024.
doi: 10.21037/jtd-24-700
**View this article at:** https://dx.doi.org/10.21037/jtd-24-700

## Introduction

Acute lung injury (ALI) and its severe manifestation, acute respiratory distress syndrome (ARDS), represent acute respiratory insufficiency or failure resulting from a range of factors affecting both intra and extra-pulmonary systems. These conditions are characterized by heightened capillary permeability, compromised alveolar gas exchange, and infiltration of pulmonary inflammatory cells, often triggered by bacterial or viral infections (1). Although great efforts have been made to improve the diagnosis and therapy, the range of clinically accessible treatments for ALI/ARDS remains restricted on supportive treatments aiming at symptom management and quality of life improvement, and the mortality rate for patients with ALI/ARDS is still as high as 40% (2,3), highlighting the urgent requirement for additional investigation and the development of innovative therapeutic strategies.

Accumulating evidence has shown that exacerbation of pulmonary edema caused by dysfunctional endothelial induced permeability of the pulmonary vascular endothelium is an important pathological feature of ALI/ARDS (4,5). The endothelium serves as a critical gateway for leukocyte infiltration into the lung parenchyma. In response to inflammatory stimuli, the integrity of the pulmonary endothelial barrier is compromised, leading to increased permeability of the pulmonary vasculature. This increased permeability leads to the exudation of edema fluid containing proteins and circulating leukocytes, including neutrophils, activated macrophages, and activated T-lymphocytes, into the interstitial and alveolar spaces, contributing to the development of acute lung injuries, pulmonary edema, and impaired gas exchange efficiency (6).

Moreover, the maintenance of endothelial barrier integrity is closely associated with complex interendothelial junctional structures, such as adhesion junctions (AJs) and tight junctions (TJs) (7,8). Among these junctions, vascular endothelial-cadherin (VE-cadherin) is the predominant component of intercellular AJs, and any abnormalities in VE-cadherin can result in weakened adhesion between vascular endothelial cells and increased permeability (9,10). Furthermore, TJs, such as claudin and occludin, play a critical role in stabilizing the tight interactions between endothelial cells and maintaining vascular homeostasis (11). Injuries to TJs of pulmonary endothelial cells may disturb lung vascular permeability and consequently lead to additional lung injury (12), too. Therefore, therapeutical strategies targeting pulmonary vascular endothelial barrier dysfunctions by reducing pulmonary vascular permeability is a logical approach to treat ALI/ARDS.

Traditional Chinese medicine (TCM) has been used

### Highlight box

**Key findings**

- Our study proved that Lianhua Qingke (LHQK) can mitigate lipopolysaccharide (LPS)-induced acute lung injury (ALI)/acute respiratory distress syndrome (ARDS) via preserving the function and integrity of the endothelial barrier both *in vivo* and *in vitro*.

**What is known and what is new?**

- LHQK has been demonstrated to exhibit multiple therapeutic efficacies in the treatment of ALI/ARDS, including modulation of the Th-mediated immune responses and inhibition of neutrophil extracellular traps formation and pyroptosis.
- We provide additional evidence to support the protective role of LHQK and its active ingredients against LPS-induced ALI/ARDS by preserving pulmonary endothelial barrier through suppression of vascular cell adhesion molecule-1 expression and maintenance of vascular endothelial-cadherin and occluding expression.

**What is the implication, and what should change now?**

- LHQK exhibits promising therapeutic potential in preventing the progression of ALI/ARDS.

for treating lung diseases, such as cold, cough, acute tracheitis and bronchitis-related ALI/ARDS for thousands of years (13-15). TCM plays multiple therapeutic effects such as inhibiting the alveolar inflammatory response, reducing oxidative stress, and protecting the vascular endothelium (16). Lianhua Qingke (LHQK) is one of such TCM consisting of 15 herbs including Mahuang, Shigao, Lianqiao, and Huangqin, among others. It has been approved by the State Food and Drug Administration (SFDA No. 2010L00120) for treating bronchitis and acute tracheitis accompanied by cough and sputum. Previous studies have shown that LHQK exhibits excellent clinical efficacy in the treatment of ALI/ARDS, including pneumonia caused by human coronaviruses (HCoVs) bacteria, lipopolysaccharide (LPS) or smoking-induced ALI/ARDS (5,17-20) by coordinating the Th-mediated immune responses to reduce levels of pro-inflammatory cytokines (17,18) and by its inhibitory effect on neutrophil extracellular traps (NETs) formation and pyroptosis (16,20). However, whether LHQK plays a protective role in improving pulmonary vascular endothelial barrier integrity and function in ALI/ARDS remains unknown. Therefore, the present study was conducted to investigate the effects and potential mechanisms of LHQK on endothelial protection in LPS-induced ALI/ARDS *in vivo* and in LPS-induced human pulmonary microvascular endothelial cells (HPMECs) injury *in vitro*. Our results indicated the therapeutic role of LHQK on LPS-induced ALI/ARDS through preserving endothelial barrier integrity and function, providing additional evidence of LHQK for its clinical use in ALI/ARDS. We present this article in accordance with the ARRIVE reporting checklist (available at https://jtd.amegroups.com/article/view/10.21037/jtd-24-700/rc).

## Methods

### *Reagent preparation*

LHQK (Lot No. 2112001) was provided by Shijiazhuang Yiling Pharmaceutical Co., Ltd. (Shijiazhuang, China). LHQK is a patented TCM composed of *Ephedra sinica* Stapf, *Forsythia suspensa* (Thunb.) Vahl, *Scutellaria baicalensis* Georgi, *Morus Alba* L., *Prunus sibirica* L., *Peucedanum praeruptorum* Dunn, *Pinellia ternate* (Thunb.) Breit., *Citrus reticulata* Blanco, *Fritillaria thunbergia* Miq., *Arctium lappa* L., *Lonicera hypoglauca* Miq., *Rheum palmatum* L., *Platycodon grandiflorus* (Jacq.) A. DC., *Glycyrrhiza uralensis* Fisch., and Gypsum fibrosum. The standard characteristic fingerprints of LHQK consist of 22 common characteristic peaks, 14 of which have been identified as: neochlorogenic acid, chlorogenic acid, cryptochlorogenic acid, isoforsythiaside, phillygenin, hesperidin, baicalin, arctiin, aloe-emodin, glycyrrhizic acid ammonium salt, rhein, emodin, chrysophanol, and physcion (17). Dexamethasone (DEX, Lot No. H41020216) was provided by Shijiazhuang Xinxiang Changle Pharmaceutical Co., Ltd. (Shijiazhuang, China). To prepare the LHQK solution for animal experiment, the LHQK tablets and DEX tablets were dissolved in phosphate-buffered saline (PBS) to prepare 0.077 and 0.155 g/mL of LHQK solution and 1 mg/mL of DEX solution. For *in vitro* experiment, the LHQK tablets were dissolved in dimethyl sulfoxide (DMSO), subjected to stirring for a duration of 1 hour, followed by sonication for an additional hour. Subsequently, the mixture was centrifuged at 8,000 rpm for 30 min. The supernatant was subsequently filtered using a 0.22 μm pore size filter. The non-toxic concentrations of 125 and 250 μg/mL LHQK were used for cellular experiments. LPS (L2880, Sigma, USA) was dissolved in PBS to 1 mg/mL as stock solution. The study was conducted in accordance with the Declaration of Helsinki (as revised in 2013).

### *Animals*

Animal experiments were performed under a project license (No. N2022172) granted by the Hebei Academy of Integrated Traditional Chinese and Western Medicine, in compliance with national guidelines for the care and use of animals. Balb/C mice (6–8 weeks, 10–22 g) were purchased from Beijing Weitong Lihua Experimental Animal Technology Co., Ltd. (Beijing, China). The mice were maintained in autoclaved cages with free access to food and water, and were housed under conditions of the temperature of 23±3 ℃, the humidity of 55%±15%, and a 12 h light/dark circle. The experiment was conducted 1 week after the mice adapted to the new environment.

### *LPS-induced ALI/ARDS model establishment*

Mice were randomly divided into five groups (n=10 per group), including control group, LPS group, LPS + LHQK low dose group (LHQK-L), LPS + LHQK high dose group (LHQK-H), and LPS + DEX group (as positive control group). The mice of the LHQK-L and LHQK-H groups received an intragastric administration of LHQK at doses

 

of 3.7 and 7.4 g/kg/d for 3 days, respectively, while mice in DEX group received intragastric administration of DEX at a dose of 5 mg/kg once a day for 3 days. After 1 h of the last administration, all animals were gas-anesthetized by 5% isoflurane (EZVET, 902-0000-522, Beijing, China), and LPS (5 mg/kg) was instilled intratracheally in LPS, LHQK-L, LHQK-H and DEX groups, while mice in the control group received an equal amount of PBS. The mice were killed 24 hours later for lung function test, fluorescein isothiocyanate-dextran (FITC-dextran) permeability assay and samples collection for additional analysis.

### *Lung function test*

Pulmonary function was measured as previously described (21). Briefly, the mice were anaesthetized before tracheostomy (via an intraperitoneal injection of sodium pentobarbital). Then, the Mouse Lung Function Instrument (DSI Buxco® PFT system, MN, USA) was used to test the functional residual capacity (FRC), resistance index (RI), mean mid expiratory flow (MMEF), the ratio of forced expiratory volume at 20 μs to forced vital capacity (FVC) ($FEV_{20}$/FVC) were measured according to the manufacturer's instructions.

### *Lung index measurement*

Lung coefficient values, defined as the ratio of lung weight to body weight, reflects increased endothelial permeability and severity of lung injury (22). After removing the mouse lungs, the blood stains on the surface of the mouse lungs were rinsed out with saline, and the lungs were weighed and recorded by placing them on an electronic scale immediately after the lungs were blotted dry with filter paper. The lung index value (%) = lung wet weight (g)/body weight (kg) × 100% (23).

### *FITC-dextran dye extravasation assay*

Lung permeability is a reflection of the intactness of the lung barrier function. To measure endothelial permeability in the lung, we performed FITC-dextran extravasation assays. In brief, FITC-dextran (20 mg/kg, 40,000 Da, HCCH7005, Sigma, USA) was injected into mice via tail vein and allowed to circulate for 60 min. Next, mice were executed and blood was taken from the eyeballs and placed in sterile eppendorf (EP) tubes. Blood supernatants were collected by spinning at 3,000 rpm for 15 min at 4 ℃ in a centrifuge (RS-28, Heraeus, USA), Blood supernatants were diluted 20-fold with PBS for additional measurement. Bronchoalveolar lavage fluid (BALF) supernatant was prepared as described in method section. Absorbance of FITC-dextran in blood supernatants and BALF was detected at 485 and 528 nm using a multifunctional enzyme (Synergy 4, Bio Tek, USA), and then quantification was determined based on a standard curve. The ratio of fluorescence intensity of FITC-dextran in BALF to the fluorescence intensity of FITC-dextran in blood serves as a measure for assessing the permeability of the pulmonary vascular endothelial barrier.

### *BALF collection and Wright-Giemsa stain*

BALF was collected by gently washing the alveoli three times with 1 mL of 4 ℃ pre-cooled PBS via tracheal intubation after the mice were anaesthetized. The collected BALF samples were centrifuged at 1,500 rpm at 4 ℃ for 5 min. The supernatant was collected for cytokine analysis and the cell pellet was used for Wright-Giemsa stain using a Wright-Giemsa stain kit (Severn, BA-4017, Beijing, China) according to the manufacturer's protocol to detect the classification and number of inflammatory cells.

### *Hematoxylin and eosin (H&E) staining*

For histopathologic examination, the left lungs of mice were perfused with 4% paraformaldehyde (PFA), and then immediately fixed in a 4% PFA solution for 48 h. Then, the lung tissues were dehydrated in gradient solutions, embedded in paraffin, sectioned and stained with a H&E (Beyotime, Shanghai, China). Finally, the slices were photographed under a fully automated biological microscope (Leica DM6000B, Wetzlar, Germany). The severity of lung injury was quantified using a semi-quantitative scoring system according to the literature (24), including the severity of the lesion in terms of the degree of aggregation of inflammatory cells in the alveolar or capillary walls, the thickening of alveolar septa or the formation of hyaline membranes, the degree of alveolar congestion, and the hemorrhage condition. Each index was scored on a 5-point scale, at last, the total score of the 4 scores was accumulated as the lung histopathology score. The table of scoring criteria is shown in *Table 1*. Subsequently, mean linear intercept (MLI) and mean alveolar number (MAN) were calculated according to the literatures (25).

**Table 1** Criteria table for scoring lung histopathology in mice with acute lung injury

| Ratings scale/points | Pathological changes |
|---|---|
| 0 | Normal lung tissue |
| 1 | Mild lung injury, less than 25% of lung tissue involved |
| 2 | Moderate lung injury, involvement of greater than 25% and less than 50% of lung tissue extent |
| 3 | Severe lung injury, involvement of greater than 50% and less than 75% of lung tissue extent |
| 4 | Extremely severe lung injury, involvement of more than 75% of the lung tissue |

### *Immunofluorescence (IF) staining and image analysis*

Lung paraffin sections were deparaffinized using xylene and ethanol gradient, followed by washing in PBS. Then the sections were treated with heated citrate buffer (pH 8.0) for antigen retrieval and washed in PBS. The sections were then blocked with 3% hydrogen peroxide for 10 min at 37 ℃ in the dark, and subsequently blocked with 5% bovine serum albumin (BSA) for 30 min at room temperature. For the IF in HPMECs, the cells were fixed with 4% PFA for 15 min, permeabilized with 0.1% Triton X-100 for 5 min, washed in PBS, and blocked with 5% BSA for 1 h, before first and second antibodies staining as previous described. Then the blocked lung sections or cells were incubated with primary antibodies at 4 ℃ overnight. Then the sections were wash for 3 times with PBS and incubated with the secondary antibodies for 50 min at room temperature in the dark. DNA was stained with 4,6-diamidino-2-phenylindole (DAPI) (Biyuntian, China). All staining results were obtained under a high-resolution fluorescence microscopy (DMi8 THUNDER, Leica, Germany). For tissue fluorescence, three randomly selected fields of view from each section were used to count the fluorescence area of VE-cadherin, occludin and vascular cell adhesion molecule-1 (VCAM-1). For the fluorescence results of HPMECs, three randomly selected fields of view were used to count the average fluorescence intensity. Each set of experiments was done in triplications. Evaluation and quantification were performed using the software ImageJ (Maryland, USA).

First antibodies used in this study include antibodies against VE-cadherin (Abcam, Cambridge, UK, ab205336, 1:1,000), occludin (Abcam, ab216327, 1:200), VCAM-1 (Abcam, ab134047, 1:1,000) and CD31/PECAM-1 (R&D Systems, Minnesota, USA, AF3628). Secondary antibodies used for this study include Donkey anti-rabbit IgG H&L (Alexa Fluor® 647, Abcam, ab150075, 1:500) and Donkey anti-goat IgG H&L (Alexa Fluor® 488, Abcam, ab150129, 1:500).

### *Enzyme-linked immunosorbent assay (ELISA)*

Supernatant of BALF was used to measure the protein levels of tumor necrosis factor (TNF)-α (Proteintech, Wuhan, China, KE10002), interleukin (IL)-1β (Proteintech, KE10003) and IL-6 (Proteintech, KE10007) using ELISA kits following the manufacturer's instructions.

### *Cell culture*

HPMECs were supplied by ScienCell Research Laboratories (USA). The cells were cultured in endothelial cell medium supplemented with 10% fetal bovine serum (FBS), 100 U/mL of penicillin and 100 μg/mL of streptomycin at 37 ℃ in a laboratory $CO_2$ incubator with a humidified atmosphere of 5% $CO_2$. HPMECs were utilized at passages 4–8 for all experiment.

### *Cell viability assay*

The cytotoxic effects of the LHQK and LPS on the viability of HPMECs were determined by the Cell Counting Kit-8 (CCK-8, Abbkine, BMU106-CN, Wuhan, China). HPMEC suspensions were split to 96-well plates at a density of $1\times10^5$ cells/mL and cultured for 24–48 h, the HPMECs were then exposed to various concentrations LPS for different times and treated with different concentrations of LHQK for 24 h. Next, 10 μL CCK-8 solution was added to each well, and the HPMECs were incubated at 37 ℃ degrees for 4 h. Finally, the absorbance at 450 nm was measured using a microplate reader (Synergy 4, Bio Tek, USA). Cell viability = (OD experimental group − OD blank group)/OD blank group × 100%. The cell viability obtained was normalized based on the absorbance of cells in the control group.

**Table 2** Antibodies used in this study

| Antibodies | Company | Dilution |
|---|---|---|
| Anti-VE-cadherin | Abcam, ab205336, Cambridge, UK | 1:1,000 |
| Anti-VE-cadherin | Abcam, ab33168, Cambridge, UK | 1:1,000 |
| Anti-Occludin | Abcam, ab216327, Cambridge, UK | 1:1,000 |
| Anti-VCAM-1 | Abcam, ab134047, Cambridge, UK | 1:1,000 |
| Anti-GAPDH | Abcam, ab181602, Cambridge, UK | 1:1,000 |
| Beta actin | Proteintech, 66009-1, Wuhan, China | 1:1,000 |
| Goat anti-rabbit IgG H&L | Abcam, ab216777, Cambridge, UK | 1:10,000 |
| Goat anti-mouse IgG H&L | Abcam, ab216772, Cambridge, UK | 1:10,000 |

VE-cadherin, vascular endothelial-cadherin; VCAM-1, vascular cell adhesion molecule-1; GAPDH, glyceraldehyde-3-phosphate dehydrogenase.

### *HPMECs transmembrane electrical resistance (TEER) assay*

To determine the effect of LHQK on the barrier dysfunction of HPMECs, HPMECs were cultured at $1.5\times10^5$ cells/well onto the inner portion of a collagen-coated Transwell membrane (pore size 0.4 μm, diameter 6.5 mm, Corning, USA) in a 24-well plate (26). The wells with an equal amount of medium in the chamber were used as control wells. When the cells were fused to 70–80%, the medium was discarded, and 100 and 600 μL of fresh complete medium were added to the upper and lower chambers, respectively. The TEER of HPMECs was detected by using a Millicell-ESR system (Millicell® ESR-2 Bedford, USA). The HPMECs were then pre-treated with 125, 250 μg/mL of LHQK HPMECs for 2 h and then added 10 μg/mL of LPS to continue incubation for 24 h. Again, the resistance values of the cellular and control chambers of each group were recorded. TEER was determined using the following formula: TEER ($\Omega\times cm^2$) = (sample well resistance value-blank well TEER value) × bottom of the upper chamber filter membrane area (0.33 $cm^2$).

### *Western blotting (WB) analysis*

Lung tissue protein and HPMECs protein were extracted using a RIPA Lysis Kit (Beyotime Biotechnology, Shanghai, China) and quantified by bicinchoninic acid (BCA) protein assay kit (Beyotime Biotechnology, P0012) according to the manufacturer's protocol. Equal amounts of total protein (20 μg) in each group were separated on sodium dodecyl sulfate-polyacrylamide gel electrophoresis (SDS-PAGE) gels and subsequently transferred to polyvinylidene difluoride (PVDF) membranes. After being blocked in goat serum proteins (LI-COR, USA) for 1 h, the membranes were incubated overnight at 4 ℃ with primary antibody. After washing three times with Tris Buffered Saline with Tween 20 (TBST), the membranes were incubated with secondary antibody at 37 ℃ for 1 h, then the membranes were scanned and analyzed with an Odyssey dual-color infrared laser imaging system (LI-COR, USA). Finally, Image J was then used to assess protein band density. The antibodies used in the experiments are shown in the *Table 2*. Glyceraldehyde-3-phosphate dehydrogenase (GAPDH) and Beta actin were used as internal control. Each experiment was repeated 3 times.

### *Network pharmacology analysis*

Targets for 14 active components were obtained using Batman 2.0 (http://bionet.ncpsb.org.cn/batman-tcm/) and SwissTargetPrediction (http://www.swisstargetprediction.ch/). Targets for acute pneumonia were obtained from GeneCards (https://www.genecards.org/) with a relevance score ≥10.00. The intersection targets of the active components and acute pneumonia were determined using the R package "Venn Diagram".

The protein-protein interaction (PPI) network of the intersecting targets was constructed using STRING (https://cn.string-db.org/). The study species was set as "Homo sapiens", and the interaction score was set to "High confidence 0.90". Disconnected nodes in the network were hidden. The PPI network was imported into Cytoscape (v3.9.0), and network analysis was performed using the

 

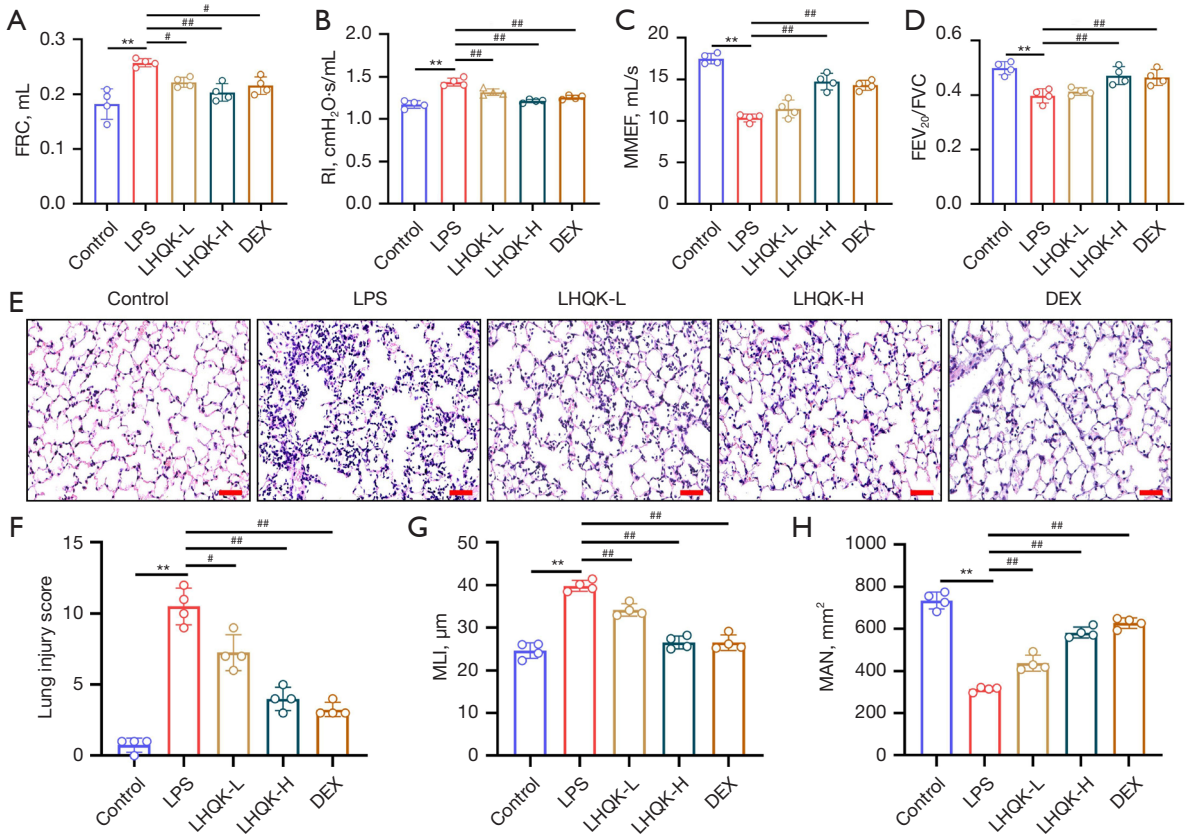


**Figure 1** LHQK prevented lung function decline in LPS-induced ALI/ARDS. FRC (A), RI (B), MMEF (C) and $FEV_{20}$/FVC (D) were measured by spirometry. (E) H&E staining of lung sections showing pathologic changes in the lungs. Scale bar: 50 μm. Lung injury scores (F), the MLI (G), and the MAN (H) were quantified. N=4 in each group. The data are expressed as mean ± SD, and statistical differences were assessed by one-way ANOVA. **, P<0.01 *vs.* the control group; #, P<0.05, ##, P<0.01 *vs.* the LPS group. FRC, functional residual capacity; RI, resistance index; MMEF, mean mid expiratory flow; $FEV_{20}$, forced expiratory volume at 20 μs; FVC, forced vital capacity; LPS, lipopolysaccharide; LHQK, Lianhua Qingke; L, low dose; H, high dose; DEX, dexamethasone; MLI, mean linear intercept; MAN, mean alveolar number; ALI, acute lung injury; ARDS, acute respiratory distress syndrome; H&E, hematoxylin and eosin; SD, standard deviation; ANOVA, analysis of variance.

"Analyse Network" tool. The CytoHubba plugin in Cytoscape was used to identify and extract the top 10 hub genes based on the Maximum Clique Centrality (MCC) algorithm. To further analyze the function of the intersection targets, Gene Ontology (GO) and Kyoto Encyclopedia of Genes and Genomes (KEGG) Enrichment Analysis were performed using the R package "clusterProfiler". The results were visualized using the "ggplot 2" package. The network of compounds-targets-biological process (BP) was constructed by Cytoscape.

### *Statistical analysis*

All statistical analyses were carried out by SPSS (version 27.0) and all graphs were created using GraphPad Prism software (version 10). Bar graphs were displayed as mean ± standard deviation. Comparisons between two groups were using the two tailed Student's *t*-test. One-way analysis of variance (ANOVA) was performed for multiple comparisons. A P value <0.05 was considered statistically significant.

## Results

### *LHQK attenuates LPS-induced lung injury*

Comprehensive observation of changes in lung function was performed on parameters, including FRC (*Figure 1A*),

RI (*Figure 1B*), MMEF (*Figure 1C*) and $FEV_{20}$/FVC (*Figure 1D*), which are tightly corelated with the air-blood exchange function of the lung. The results showed a significantly higher of FRC and RI (P<0.01) and a significantly lower of MMEF and $FEV_{20}$/FVC in LPS group mice compared with the control group (P<0.01). In contrast, FRC (LHQK-L, DEX: P<0.05; LHQK-H: P<0.01) and RI (P<0.01) were significantly reduced after LHQK and DEX treatment, whereas MMEF and $FEV_{20}$/FVC were significantly elevated (P<0.01) in LHQK-H and DEX groups.

Next, H&E staining (*Figure 1E*) and relatively lung injury score (*Figure 1F*) as well as MLI (*Figure 1G*) and MAN (*Figure 1H*) quantification were performed to evaluate the morphological and pathological changes of lung tissues. These results revealed that lung injuries, including enlarged alveoli, thickening of alveolar walls, accompanied by inflammatory cell infiltration in the alveolar lumen and interalveolar space (*Figure 1E*), increased lung injury score and alveolar size (P<0.01) (*Figure 1F,1G*), and decreased alveolar number (P<0.01) (*Figure 1H*) were found in the LPS group, suggesting that the ALI/ARDS model was successfully established. Following treatment with LHQK and DEX, ameliorated lung parenchymal lesions and inflammatory cell infiltration were observed (*Figure 1E*). Moreover, LHQK and DEX significantly reduced the LPS-induced lung injury score (LHQK-L: P<0.05; LHQK-H, DEX: P<0.01) (*Figure 1F*) and significantly reduced alveolar size (P<0.01) and the number of alveoli was significantly increased (P<0.01) (*Figure 1G,1H*).

### *LHQK suppresses LPS-induced pulmonary inflammation and down-regulates VCAM-1 in lung of mice with ALI/ARDS*

To further investigate the effect of LHQK on LPS-induced inflammation, BALF was collected for Wright-Giemsa staining (*Figure 2A*), immune cell quantification (*Figure 2B-2D*) and pro-inflammatory cytokine analysis (*Figure 2E-2G*). The results showed that the BALF samples from the control group mice contained a small amount of immune cells, while the numbers of total cells, macrophages, and neutrophils were significantly increased in the LPS group, compared to the control group (P<0.01) (*Figure 2A-2D*). However, LHQK and DEX effectively inhibited the LPS-induced increases in these cells (P<0.01) (*Figure 2A-2D*). Moreover, pro-inflammatory cytokines, includes TNF-α (*Figure 2E*), IL-1β (*Figure 2F*) and IL-6 (*Figure 2G*) were analyzed using ELISA. Compared to the control group, levels of TNF-α, IL-1β and IL-6 were significantly elevated in the LPS group (P<0.01), but significantly reduced upon LHQK and DEX treatment (P<0.01) (*Figure 2E-2G*).

Since adhesion molecules, such as VCAM-1, play a critical role in pulmonary inflammation caused by LPS stimulation (27,28). We next investigated the expression level of VCAM-1 by IF staining (*Figure 2H,2I*) and western blot (*Figure 2J,2K*). Both of the results of IF staining and western blot results indicated that the expression of VCAM-1 was significantly elevated in the lungs of the LPS group compared to the control group (P<0.01), while significantly down regulated in the lungs of LHQK and DEX the expression of adhesion molecules when compared to the LPS group (LHQK-L: P<0.05; LHQK-H, DEX: P<0.01) (*Figure 2H-2K*). Together, these results indicate that LHQK attenuates pulmonary inflammation probably by inhibiting the upregulation of VCAM-1 induced by LPS in ALI/ARDS mice, therefore suppressing the recruitment of inflammatory cells infiltration to the lung.

### *LHQK ameliorates pulmonary edema and permeability of pulmonary vessels by protecting endothelial barrier in LPS-induced ALI/ARDS mice*

In order to assess the effects of LPS and LHQK on the pulmonary vascular endothelial barrier function, lung coefficient values (22) (*Figure 3A*) as well as FITC-dextran extravasation assays (*Figure 3B*) were performed to evaluate the pulmonary edema and endothelial permeability in the lung. Compared with the control group, the LPS group showed a significantly higher coefficient value (P<0.01) (*Figure 3A*) and a higher concentration of FITC-dextran detected in lung tissues (P<0.01) (*Figure 3B*), demonstrating pulmonary edema and an increased pulmonary barrier permeability. However, pulmonary edema and pulmonary vascular leakage were significantly suppressed after treatment by LHQK and DEX (P<0.01) (*Figure 3A,3B*).

Given that abnormal endothelial junctions including AJs and TJs are the major cause of impaired pulmonary vascular endothelial barrier, a typical pathological feature of ALI/ARDS, therefore, we next examined the expression of VE-cadherin (*Figure 4A-4D*), an AJ protein, and occludin (*Figure 4E-4H*), a core TJ, by both immunofluorescent staining and western blot in lung samples of our experiment. The IF results of VE-cadherin demonstrated that, when compared to the control group, the level of VE-cadherin protein expression was significantly lower in the lungs of the LPS group (P<0.01), whereas LHQK and DEX significantly

 

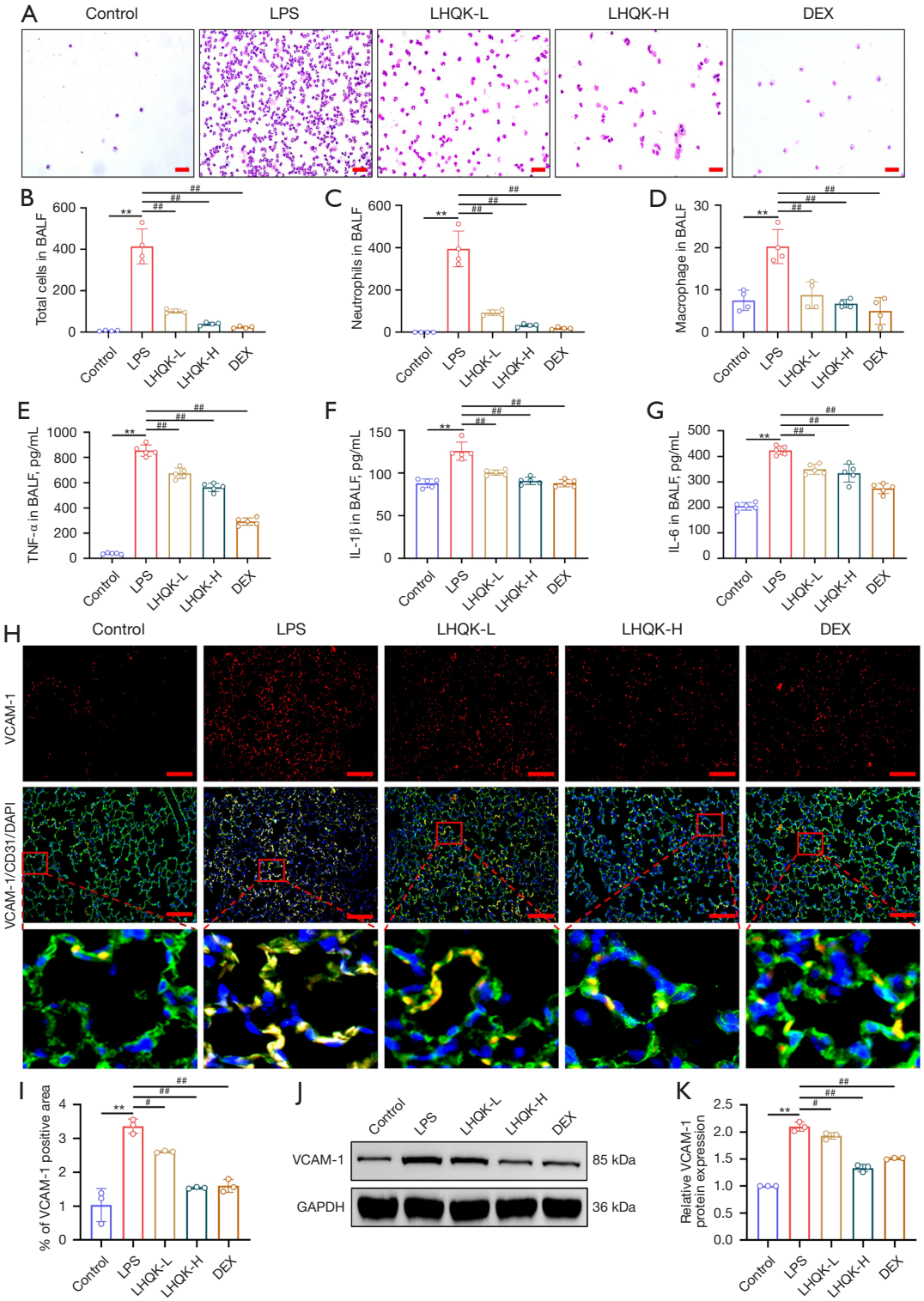


**Figure 2** LHQK suppresses LPS-induced pulmonary inflammation and down-regulates VCAM-1 in lung of mice with ALI/ARDS. (A) Wright-Giemsa staining (magnification ×200). Scale bar, 50 μm. (B-D) Total number of inflammatory cells, number of neutrophils, number of macrophages changes. (E-G) ELISA for TNF-α, IL-1β and IL-6 expression levels in mouse BALF. (H,I) VCAM-1 (red) co-stained with CD31 (green) and DAPI (blue) in immunofluorescence (H) and the quantification results (I). Scale bars: 100 μm. (J,K) Representative

western blot images of VCAM-1 (J) and corresponding quantitative analyses (K). N=4 in each group. The data are expressed as mean ± SD, and statistical differences were assessed by one-way ANOVA. **, P<0.01 *vs.* the control group; #, P<0.05, ##, P<0.01 *vs.* the LPS group. LPS, lipopolysaccharide; LHQK, Lianhua Qingke; L, low dose; H, high dose; DEX, dexamethasone; BALF, bronchoalveolar lavage fluid; TNF, tumor necrosis factor; IL, interleukin; VCAM-1, vascular cell adhesion molecule-1; DAPI, 4,6-diamidino-2-phenylindole; ALI, acute lung injury; ARDS, acute respiratory distress syndrome; ELISA, enzyme-linked immunosorbent assay; SD, standard deviation; ANOVA, analysis of variance.

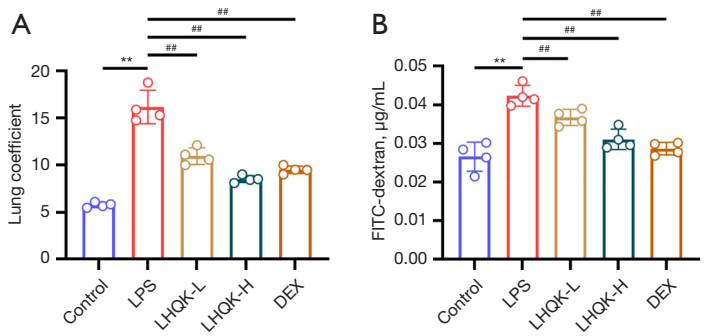


**Figure 3** LHQK ameliorates LPS-induced pulmonary edema and increased permeability of pulmonary vessels. (A) Lung coefficient ratio. (B) Lung tissue FITC-dextran exudation. N=4 in each group. The data are expressed as mean ± SD, and statistical differences were assessed by one-way ANOVA. **, P<0.01 *vs.* the control group; ##, P<0.01 *vs.* the LPS group. LPS, lipopolysaccharide; LHQK, Lianhua Qingke; L, low dose; H, high dose; DEX, dexamethasone; FITC, fluorescein isothiocyanate; SD, standard deviation; ANOVA, analysis of variance.

increased the expression of VE-cadherin (P<0.01) (*Figure 4A*,*4B*). Similarly, western blot analysis revealed that the expression level of VE-cadherin is significantly down regulated in mouse lung tissues after LPS stimulation (P<0.01) but up-regulated upon LHQK and DEX treatment (LHQK-L: P<0.05; LHQK-H, DEX: P<0.01) (*Figure 4C*,*4D*). Further, IF immunofluorescent staining as well as western blot of occludin and their quantification results revealed that the level of occludin protein expression was significantly lower in the lungs of the LPS group compared to the control group (P<0.01) (*Figure 4E-4H*). While, compared to the LPS group, LHQK and DEX significantly increased the expression of occludin (LHQK-L: P<0.05; LHQK-H, DEX: P<0.01) (*Figure 4E-4H*). Collectively, all these results demonstrated that LHQK exists a potential to ameliorate pulmonary edema and permeability probably by preventing endothelial cell apoptosis and maintaining the levels of VE-cadherin and occludin that are critical for the integrity of endothelial barrier.

### *LHQK protects against LPS-induced HPMECs barrier disruption in vitro*

To further investigate the effect of LHQK on LPS-induced endothelial barrier dysfunction *in vitro*, an HPMECs injury model induced by LPS was established. Upon to the cell viability optimization results, 10 μg/mL LPS treatment for 24 h, with 50% cell viability, was chosen for HPMEC injury model (*Figure 5A*) and the non-toxic concentration of 1, 50, 125 and 250 μg/mL (*Figure 5B*). Moreover, we found that LHQK treatment at 50, 125 and 250 μg/mL attenuated the reduction in cell viability effectively, therefore 125 and 250 μg/mL were selected as the optimal therapeutic concentrations of LHQK-L and LHQK-H for cellular experiments in this study (P<0.01) (*Figure 5C*).

Next, TEER values analysis was used to assess the permeability of HPMECs monolayer (*Figure 5D*). The results showed that the TEER value of LPS treatment group was significantly lower than that in the control group (P<0.01), suggesting that LPS disrupts the endothelial barrier integrity of HPMECs. Of note, the reduction of the TEER value was significantly improved after treatment with LHQK (P<0.01).

In addition, the expression levels of VE-cadherin protein by IF and western blot consistently showed that the expression level of VE-cadherin was significantly reduced in the LPS group compared with the control group (P<0.01), but was significantly increased after

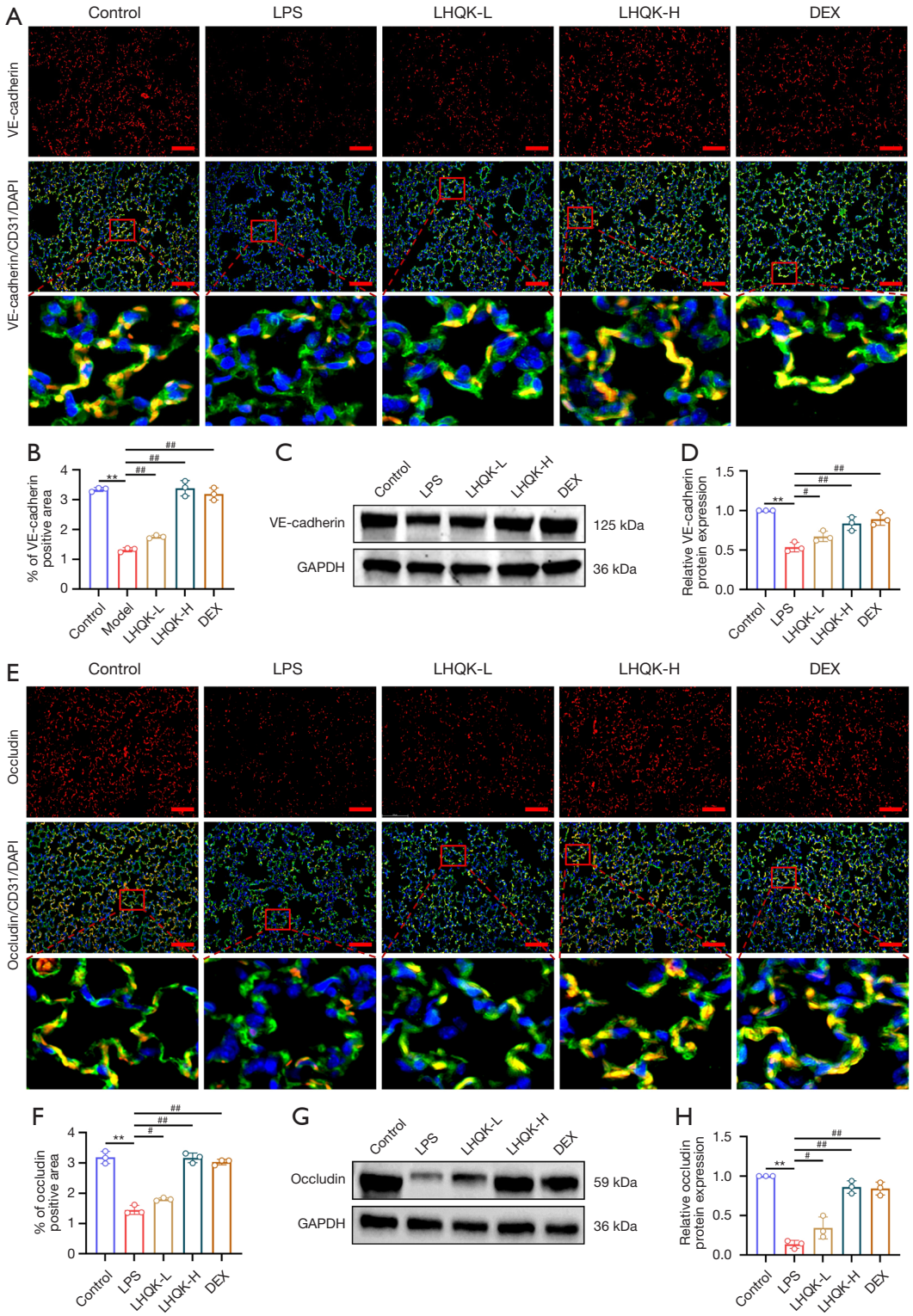


**Figure 4** LHQK inhibits the LPS-induced down-regulation of endothelial junction proteins in mouse lung tissue. (A,B) Immunofluorescence staining of VE-cadherin (red) co-stained with CD31 (green) and DAPI (blue) (A) and quantification results of fluorescence area of VE-cadherin (B). Scale bar: 100 μm. (C,D) Representative western blot images of VE-cadherin (C) and corresponding quantitative analyses (D). (E,F) Immunofluorescence staining of occludin (red) co-stained with CD31 (green) and DAPI (blue) (E) and

quantification results of fluorescence area of occludin (F). Scale bar: 100 μm. (G,H) Representative western blot images of occludin (G) and corresponding quantitative analyses (H). N=3 in each group. The data are expressed as mean ± SD, and statistical differences were assessed by one-way ANOVA. **, P<0.01 *vs.* the control group; #, P<0.05, ##, P<0.01 *vs.* the LPS group. LPS, lipopolysaccharide; LHQK, Lianhua Qingke; L, low dose; H, high dose; DEX, dexamethasone; VE-cadherin, vascular endothelial-cadherin; DAPI, 4,6-diamidino-2-phenylindole; SD, standard deviation; ANOVA, analysis of variance.

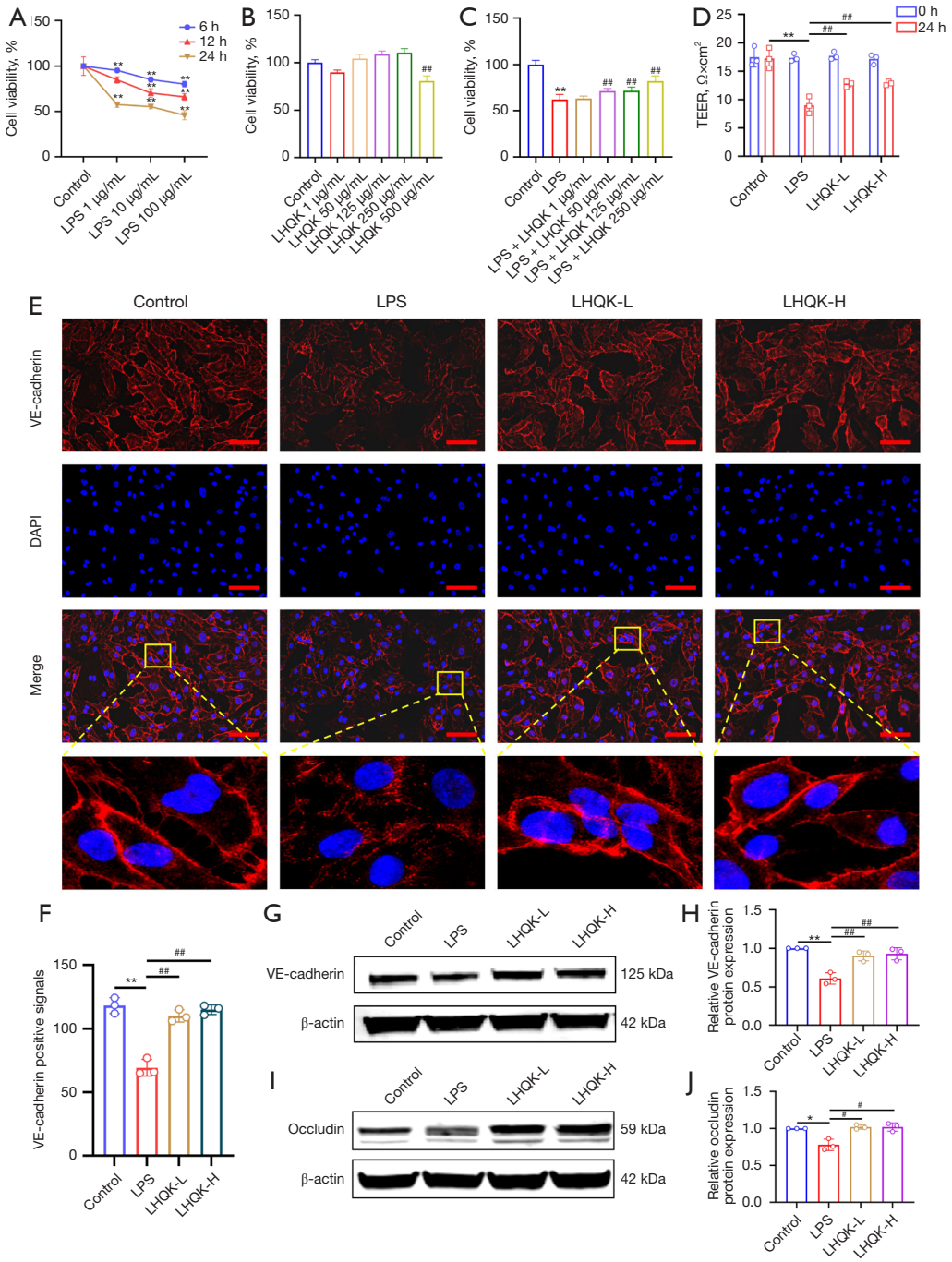


**Figure 5** LHQK inhibits LPS-induced decrease in transmembrane resistance values and increase in permeability of HPMECs. (A) Effects of exposure to different concentrations and times of LPS on the viability of HPMECs. (B) Toxic effects of different concentrations of

LHQK on HPMEC cells. (C) Viability of HPMECs exposed to LPS with or without LHQK treatment. (D) Experimental results of TEER values. (E,F) Immunofluorescence staining of VE-cadherin (red) co-stained with DAPI (blue) (E) and corresponding quantitative analyses (F). Scale bar: 100 μm. (G,H) Representative western blot images of VE-cadherin (G) and corresponding quantitative analyses (H). (I,J) Representative western blot images of occludin (I) and corresponding quantitative analyses (J). The data are expressed as mean ± SD, and statistical differences were assessed by one-way ANOVA. *, P<0.05, **, P<0.01 *vs.* the control group; #, P<0.05, ##, P<0.01 *vs.* the LPS group. LPS, lipopolysaccharide; LHQK, Lianhua Qingke; L, low dose; H, high dose; TEER, transepithelial electrical resistance; VE-cadherin, vascular endothelial-cadherin; DAPI, 4,6-diamidino-2-phenylindole; HPMECs, human pulmonary microvascular endothelial cells; SD, standard deviation; ANOVA, analysis of variance.

the administration of LHQK (P<0.01) (*Figure 5E-5H*). Similarly as the previous results in the lung, western blot results showed that the expression level of occludin was significantly reduced in the LPS group (P<0.05), which was significantly ameliorated upon LHQK administration (P<0.05) (*Figure 5I,5J*). All together, these results demonstrate that LHQK protects LPS-induced HPMECs monolayer permeability by preserving the protein levels of VE-cadherin and occludin.

### *LHQK's active ingredients exhibit protective potential in preserving the integrity of the endothelial barrier*

To explore the basis of LHQK action on endothelial protection, a network pharmacological analysis was performed to predict the potential active ingredients of LHQK on endothelial protection by using fourteen components identified from LHQK tablets by Wang *et al.* (17), including neochlorogenic acid, chlorogenic acid, cryptochlorogenic acid, isoforsythiaside, phillygenin, hesperidin, baicalin, arctiin, aloe-emodin, glycyrrhizic acid ammonium salt, rhein, emodin, chrysophanol, and physcion. A total of 890 target genes of 14 active components were screened using Batman 2.0, and an additional 526 target genes were retrieved from Swiss Target Prediction. By combining and removing duplicates, a total of 1,293 target genes of the 14 active components were obtained. GeneCards identified 496 target genes associated with acute pneumonia. Among these, 205 target genes were found to intersect with the 14 active components (*Figure 6A*). The PPI network of these 205 intersection targets is depicted in (*Figure 6B*), which consisted of 185 nodes and 931 edges. The color intensity of the nodes deepened as the degree value increased. The top 10 hub genes extracted from the PPI network were *IL-6*, *TNF*, *IL-1*β, *IL-1A*, *IFNG*, *CXCL10*, *IL-10*, *CCL5*, *CSF2* and *IL-4* (*Figure 6C*). To evaluate the mechanisms of LHQK in acute pneumonia, GO and KEGG enrichment analyses were performed. The results of GO enrichment analysis revealed that the BP terms were mainly associated with "regulation of cell-cell adhesion", "vascular endothelial growth factor signaling pathway", and "establishment of endothelial barrier" (*Figure 6D*). The KEGG enrichment analysis results indicated that the intersection targets were primarily enriched in signaling pathways such as "TNF signaling pathway", "Coronavirus disease-COVID-19", "IL-17 signaling pathway", "Apoptosis", "Focal adhesion" and "Adherens junction". These findings suggest that the potential mechanism of active ingredients of LHQK in acute pneumonia may involve the regulation of endothelial cell adhesion, inflammation and apoptosis signaling pathways (*Figure 6E*).

To further evaluated the TJ expression regulation, thirteen components out of those active ingredients identified from LHQK (17) were optimized for their maximal non-toxic concentration by cell viability assay and used for subsequent analysis (*Figure 7A*). Moreover, screening in LPS treated HPMECs showed that active compounds, including baicalin, arctiin, physcion, glycyrrhizate, neochlorogenic acid, chrysophanol, cryptochlorogenic acid, chlorogenic acid, rhein and isoforsythiaside, exhibit endothelial protective probability (*Figure 7B*).

Finally, western blot and quantitative analysis were used to screen the active compounds that regulate the expression levels of occludin in LPS-induced HPMECs injury model. The results showed that the decreased protein levels of occludin induced by LPS were attenuated upon treatment with seven active ingredients, including chrysophanol (DHF), neochlorogenic acid (XLYS), baicalin (HQG), cryptochlorogenic acid (YLYS), rhein (DHS), isoforsythiaside (YLQG), chlorogenic acid (LYS), physcion (DHSJM), arctiin (NBZG) and glycyrrhizic acid ammonium salt (GCSDAY) (P<0.05 or P<0.01) (*Figure 8A,8B*).

## Discussion

This study aimed to investigate the role and underlying

 

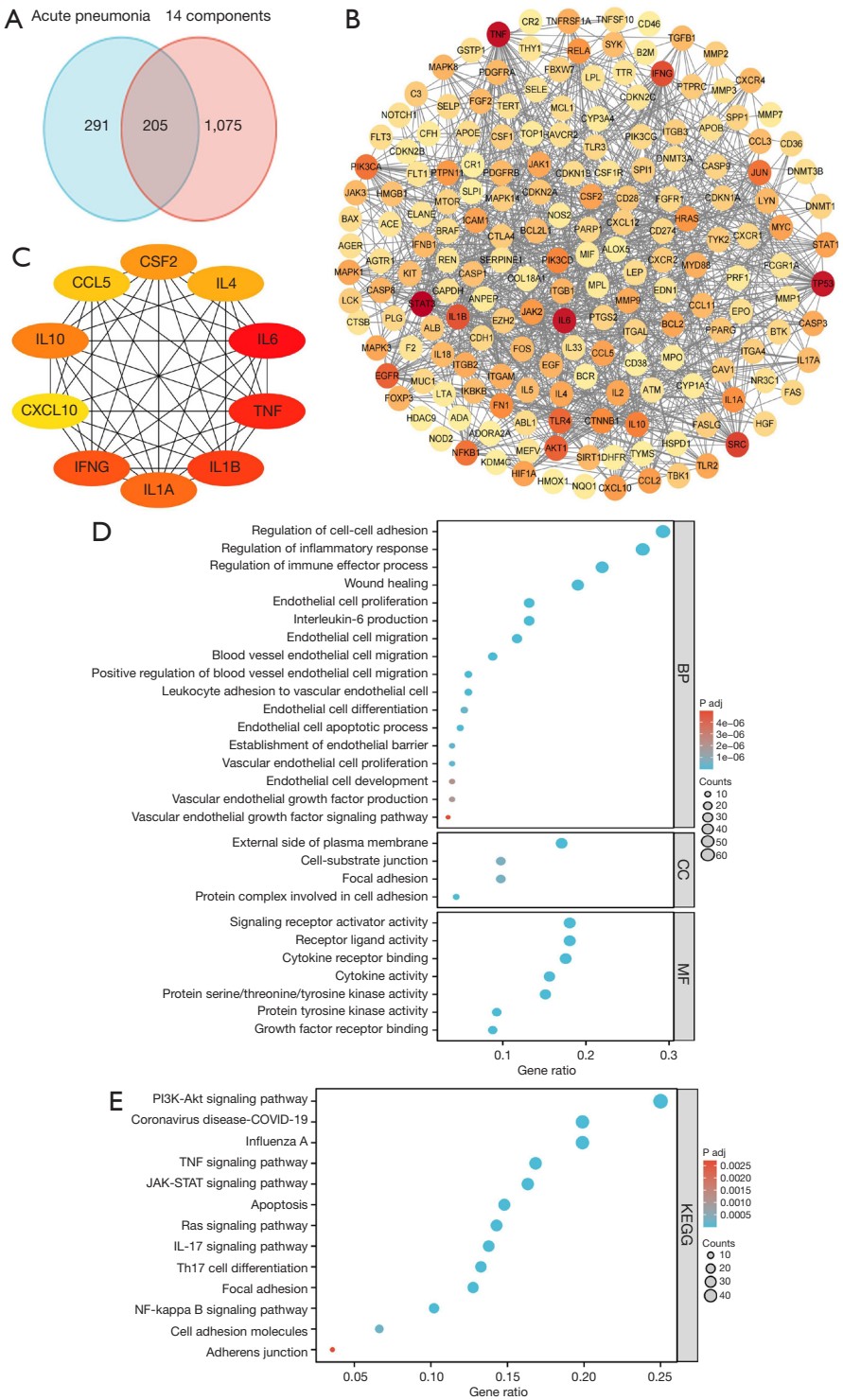


**Figure 6** The results of network pharmacological analysis. (A) Venn diagram of the targets. (B) The PPI network of 205 targets. (C) The subnetwork of top 10 genes. (D) The bubble chart of GO enrichment analysis result. (E) The bubble chart of KEGG enrichment analysis result. BP, biological process; CC, cellular component; MF, molecular function; COVID-19, coronavirus disease 2019; TNF, tumor necrosis factor; JAK-STAT, Janus kinase-signal transducers and activators of transcription; IL, interleukin; NK, natural killer; KEGG, Kyoto Encyclopedia of Genes and Genomes; PPI, protein-protein interaction; GO, Gene Ontology.

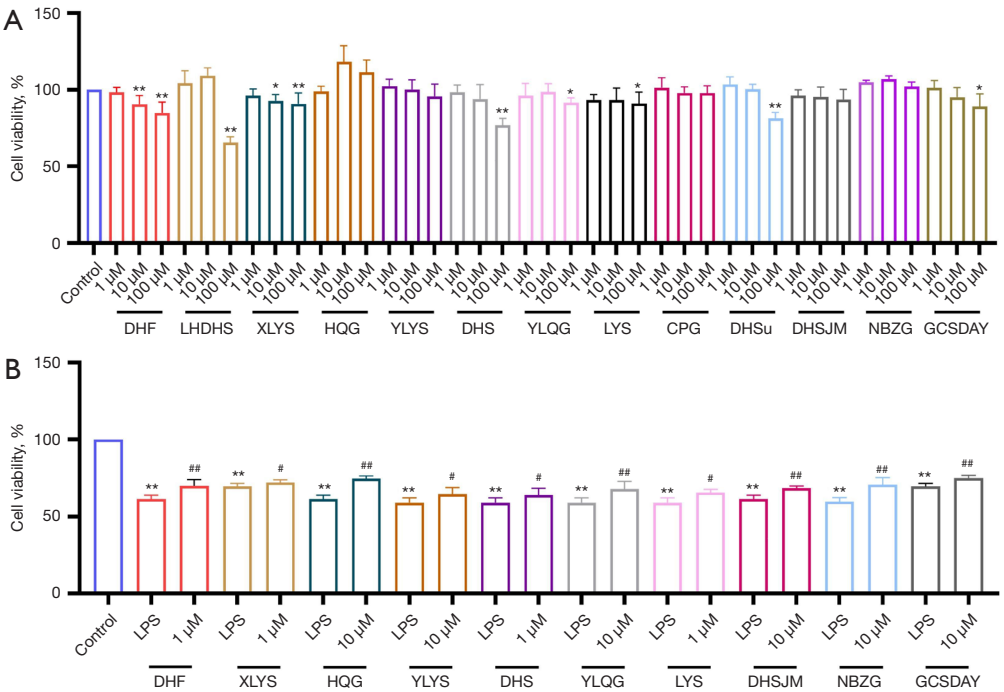


**Figure 7** Cell viability of active gradients of LHQK on HPMECs. (A) Effect of different concentrations of active gradients on cell viability. The maximal non-toxic concentration for major of them are 100 μM, except for chrysophanol 10 and 100 μM, neochlorogenic acid 10 and 100 μM, rhein 100 μM, isoforsythiaside 100 μM, glycyrrhizic acid ammonium salt 100 μM, aloe-emodin 100 μM, emodin 100 μM and chlorogenic acid 100 μM. (B) Viability of HPMECs exposed to LPS with or without active ingredient treatment. The concentrations of active ingredients were chrysophanol (DHF) 1 μM, neochlorogenic acid (XLYS) 1 μM, baicalin (HQG) 10 μM, cryptochlorogenic acid (YLYS) 1 μM, rhein (DHS) 1 μM, isoforsythiaside (YLQG) 10 μM, chlorogenic acid (LYS) 1 μM, physcion (DHSJM) 10 μM, arctiin (NBZG) 10 μM and glycyrrhizic acid ammonium salt (GCSDAY) 10 μM. The data are expressed as mean ± SD, and statistical differences were assessed by one-way ANOVA. *, P<0.05, **, P<0.01 *vs.* the control group; #, P<0.05, ##, P<0.01 *vs.* the LPS group. LPS, lipopolysaccharide; LHQK, Lianhua Qingke; HPMECs, human pulmonary microvascular endothelial cells; SD, standard deviation; ANOVA, analysis of variance.

mechanism of LHQK on pulmonary vascular endothelial barrier integrity and function in models of LPS-induced ALI/ARDS *in vivo* and LPS-induced HPMECs injury *in vitro*. We proved that LHQK could effectively improve LPS-induced lung function decline, lung histopathological injury, inflammatory cells infiltration, cytokine production, pulmonary edema, pulmonary vascular permeability *in vivo*, and attenuate LPS-induced cell-permeability of HPMECs *in vitro*. In addition, we have demonstrated the regulatory effect of LHQK on several critical proteins that exhibit a strong correlation with the functionality and integrity of the endothelial barrier. These proteins include VCAM-1, which plays critical role in the recruitment of inflammatory cells, and endothelial junctions such as VE-cadherin and occludin. Finally, we predicted and identified the potential active ingredient of LHQK that exhibits a protective effect on HPMECs against LPS-induced injury. Our findings collectively indicate that LHQK and its active components play a protective role in preserving the function and integrity of the endothelial barrier both *in vivo* and *in vivo*.

The main clinical manifestations of ALI/ARDS are pulmonary edema and severe inflammatory responses in the lungs (29). Firstly, LPS stimulation induces the release of pro-inflammatory factors, such as TNF-α, IL-1β, and IL-6, which leads to the disruption of paracellular junctions (30,31), thus affecting multiple processes of ALI. Secondly, LPS promotes the secretion of the adhesion molecule VCAM-1 from the vascular endothelium to recruit leukocytes to elicit an inflammatory response, thereby increasing pulmonary vascular endothelial permeability and pulmonary edema (32). The present study confirmed that LHQK treatment could effectively reduce the levels of pro-

 

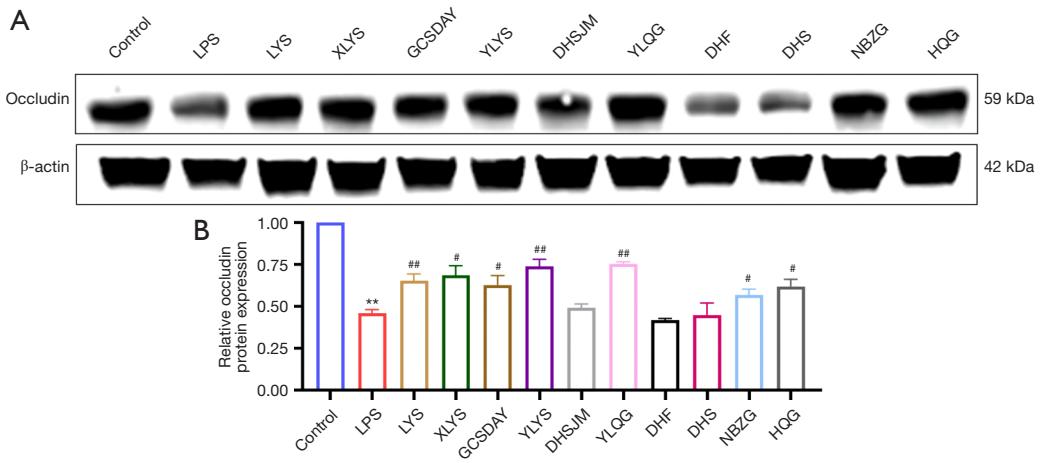


**Figure 8** Effective active components of LHQK on the expression levels of tight junction proteins in HPMEC cells. (A,B) Representative western blot images of occludin (A) and corresponding quantitative analyses (B), including chlorogenic acid (LYS), neochlorogenic acid (XLYS), glycyrrhizic acid ammonium salt (GCSDAY), cryptochlorogenic acid (YLYS), physcion (DHSJM), isoforsythiaside (YLQG), chrysophanol (DHF), rhein (DHS), arctiin (NBZG), baicalin (HQG). N=3 in each group. The data are expressed as mean ± SD, and statistical differences were assessed by one-way ANOVA. **, P<0.01 *vs.* the control group; #, P<0.05, ##, P<0.01 *vs.* the LPS group. LPS, lipopolysaccharide; LHQK, Lianhua Qingke; HPMECs, human pulmonary microvascular endothelial cells; SD, standard deviation; ANOVA, analysis of variance.

inflammatory cytokines and downregulate the expression of VCAM-1, therefore, contributing to the reduction of inflammatory cell infiltration.

Moreover, study has shown that LPS can directly disrupts endothelial barrier function, which leads to increased vascular permeability and increased pulmonary edema (33). The results of this study showed that the lung coefficient ratio and the extravasation rate of FITC-dextran in lung tissues were significantly reduced in LHQK administrated group, consistently the TEER assay results *in vitro* confirmed the protective role of LHQK on alleviating LPS-induced HPMECs permeability, too. It has been proved that the pulmonary vascular barrier is mainly regulated by tight and adhesive connections between vascular endothelial cells (34). Among which, VE-cadherin and occludin play a crucial role in maintaining endothelial barrier integrity, respectively (35,36). In this study, we showed that LHQK significantly upregulated the expression levels of both VE-cadherin and occludin in both lung tissues of ALI/ARDS mice and in LPS treated HPMECs, confirming a role of LHQK on protecting endothelial barrier integrity via regulating the expression levels of TJ proteins and adhesion proteins.

Previous studies have proved the therapeutic effects and mechanisms of LHQK on relieving airway mucus hypersecretion (37) by maintaining airway epithelial homeostasis, ameliorating HCoV-induced pneumonia by decreasing the levels of pro-inflammatory cytokines through orchestrating Th-mediated immune responses (17) and alleviating LPS-induced pulmonary ALI/ARDS by inhibiting NETs formation and pyroptosis (20). Other than that, our *in vivo* and *in vitro* experiments revealed the diverse pharmacological properties of LHQK in protecting pulmonary endothelial barrier injuries induced by LPS through inhibiting VCAM-1 regulated inflammatory cell infiltration, particularly VE-cadherin and occludin regulated integrity and permeability of endothelial barrier, supporting the advantage of TCM in treating disease with multiple components, multiple targets and multiple pathways.

Finally, we have made effort to identify the potential active ingredients of LHQK on endothelial cell protection based on those identified in published LHQK ultra-performance liquid chromatography-tandem mass spectrometry (UPLC-MS/MS) data by pharmacological network analysis and cellular screening. However, more future research combined with pharmacodynamic analysis of LHQK should be performed to decipher the pharmacological mechanism and molecular basis of LHQK in endothelial cell protection property in anti-ALI/ARDS.

## Conclusions

In summary, LHQK can mitigate LPS-induced inflammatory infiltration, pulmonary edema, and pulmonary vascular endothelial barrier dysfunction in the context of ALI/ARDS. This is achieved by decreasing the levels of VCAM-1, and increasing the expression levels of barrier-associated junctions, such as VE-cadherin and occluding. Consequently, LHQK exhibits promising therapeutic potential in preventing the progression of ALI/ARDS.

## Acknowledgments

*Funding:* This work was supported by the Innovation Team and Talents Cultivation Program of National Administration of Traditional Chinese Medicine (No. ZYYCXTD-D-202206), Key Project of National Natural Science Foundation of China (No. 82130123), Natural Science Foundation of Hebei Province (No. H2023106039), Hebei Provincial Innovation Ability Improvement Program (No. 225A2503D), Scientific Research Project of Hebei Provincial Administration of Traditional Chinese Medicine (No. 2024401), and S&T Program of Hebei Province (No. 23372508D).

## Footnote

*Reporting Checklist:* The authors have completed the ARRIVE reporting checklist. Available at https://jtd.amegroups.com/article/view/10.21037/jtd-24-700/rc

*Data Sharing Statement:* Available at https://jtd.amegroups.com/article/view/10.21037/jtd-24-700/dss

*Peer Review File:* Available at https://jtd.amegroups.com/article/view/10.21037/jtd-24-700/prf

*Conflicts of Interest:* All authors have completed the ICMJE uniform disclosure form (available at https://jtd.amegroups.com/article/view/10.21037/jtd-24-700/coif). Z.J. is the spouse of Ms. Rui Wu, who holds shares and serves as a director of Shijiazhuang Yiling Pharmaceutical Co., Ltd. Z.J. reports affiliated to Hebei Yiling Hospital, a non-profit medical institution, which is two completely independent legal entities with Shijiazhuang Yiling Pharmaceutical Co., Ltd. He has fully disclosed these interests to the research committee and have developed an approved plan to manage any potential conflicts that may arise from such an arrangement and ensure the research results being scientific, objective and authoritative. The other authors have no conflicts of interest to declare.

*Ethical Statement:* The authors are accountable for all aspects of the work in ensuring that questions related to the accuracy or integrity of any part of the work are appropriately investigated and resolved. The study was conducted in accordance with the Declaration of Helsinki (as revised in 2013). Animal experiments were performed under a project license (No. N2022172) granted by the Hebei Academy of Integrated Traditional Chinese and Western Medicine, in compliance with national guidelines for the care and use of animals.



## References

1. Shah RD, Wunderink RG. Viral Pneumonia and Acute Respiratory Distress Syndrome. Clin Chest Med 2017;38:113-25.
2. Nelin LD, Jin Y, Chen B, et al. Cyclooxygenase-2 deficiency attenuates lipopolysaccharide-induced inflammation, apoptosis, and acute lung injury in adult mice. Am J Physiol Regul Integr Comp Physiol 2022;322:R126-35.
3. Fu C, Hao S, Xu X, et al. Activation of SIRT1 ameliorates LPS-induced lung injury in mice via decreasing endothelial tight junction permeability. Acta Pharmacol Sin 2019;40:630-41.
4. Wu Y, Yu X, Wang Y, et al. Ruscogenin alleviates LPS-triggered pulmonary endothelial barrier dysfunction through targeting NMMHC IIA to modulate TLR4 signaling. Acta Pharm Sin B 2022;12:1198-212.
5. Liu MM, Zhou J, Ji D, et al. Diammonium glycyrrhizinate lipid ligand ameliorates lipopolysaccharide-induced acute lung injury by modulating vascular endothelial barrier function. Exp Ther Med 2021;21:303.
6. Chambers E, Rounds S, Lu Q. Pulmonary Endothelial

Cell Apoptosis in Emphysema and Acute Lung Injury. Adv Anat Embryol Cell Biol 2018;228:63-86.
7. Baluk P, McDonald DM. Buttons and Zippers: Endothelial Junctions in Lymphatic Vessels. Cold Spring Harb Perspect Med 2022;12:a041178.
8. Englert JA, Macias AA, Amador-Munoz D, et al. Isoflurane Ameliorates Acute Lung Injury by Preserving Epithelial Tight Junction Integrity. Anesthesiology 2015;123:377-88.
9. Xiong S, Hong Z, Huang LS, et al. IL-1β suppression of VE-cadherin transcription underlies sepsis-induced inflammatory lung injury. J Clin Invest 2020;130:3684-98.
10. Wettschureck N, Strilic B, Offermanns S. Passing the Vascular Barrier: Endothelial Signaling Processes Controlling Extravasation. Physiol Rev 2019;99:1467-525.
11. Barral M, Boudour S, Viprey M, et al. Stent retriever thrombectomy for acute ischemic stroke: A systematic review and meta-analysis of randomized controlled trials, including THRACE. Rev Neurol (Paris) 2018;174:319-26.
12. Godbole NM, Chowdhury AA, Chataut N, et al. Tight Junctions, the Epithelial Barrier, and Toll-like Receptor-4 During Lung Injury. Inflammation 2022;45:2142-62.
13. Chen YB, Liu Q, Xie H, et al. Is Chinese Medicine Injection Applicable for Treating Acute Lung Injury and Acute Respiratory Distress Syndrome? A Systematic Review and Meta-analysis of Randomized Controlled Trials. Chin J Integr Med 2020;26:857-66.
14. Li GH, Sun XJ, Deng YH, et al. Meta-analysis and trial sequential analysis of Qingjin Huatan Decoction for treating community-acquired pneumonia in elderly. Zhongguo Zhong Yao Za Zhi 2020;45:2658-67.
15. Zheng W, Huang X, Lai Y, et al. Glycyrrhizic Acid for COVID-19: Findings of Targeting Pivotal Inflammatory Pathways Triggered by SARS-CoV-2. Front Pharmacol 2021;12:631206.
16. Yu WY, Gao CX, Zhang HH, et al. Herbal Active Ingredients: Potential for the Prevention and Treatment of Acute Lung Injury. Biomed Res Int 2021;2021:5543185.
17. Wang M, Li W, Cui W, et al. The therapeutic promises of Lianhuaqingke in the mice model of coronavirus pneumonia (HCoV-229E and SARS-CoV-2). Chin Med 2021;16:104.
18. Zhang L, Wu L, Xu X, et al. Efficacy and Safety of Lianhua Qingke Tablets in the Treatment of Mild and Common-Type COVID-19: A Randomized, Controlled, Multicenter Clinical Study. Evid Based Complement Alternat Med 2022;2022:8733598.
19. Jin L, Xu Y, Yuan H. Effects of four types of integrated Chinese and Western medicines for the treatment of COVID-19 in China: a network meta-analysis. Rev Assoc Med Bras (1992) 2020;66:771-7.
20. Peng W, Qi H, Zhu W, et al. Lianhua Qingke ameliorates lipopolysaccharide-induced lung injury by inhibiting neutrophil extracellular traps formation and pyroptosis. Pulm Circ 2023;13:e12295.
21. Haw TJ, Starkey MR, Pavlidis S, et al. Toll-like receptor 2 and 4 have opposing roles in the pathogenesis of cigarette smoke-induced chronic obstructive pulmonary disease. Am J Physiol Lung Cell Mol Physiol 2018;314:L298-317.
22. Kosutova P, Mikolka P, Balentova S, et al. Effects of phosphodiesterase 5 inhibitor sildenafil on the respiratory parameters, inflammation and apoptosis in a saline lavage-induced model of acute lung injury. J Physiol Pharmacol 2018.
23. Bao YY, Shi YJ, Guo SS, et al. Study on therapeutic effect of Chaiyin Particles on combining disease with syndrome of human coronavirus pneumonia with pestilence attacking lung syndrome based on regulation of immune function. Zhongguo Zhong Yao Za Zhi 2020;45:3020-7.
24. Liu T, Zhou Y, Li P, et al. Blocking triggering receptor expressed on myeloid cells-1 attenuates lipopolysaccharide-induced acute lung injury via inhibiting NLRP3 inflammasome activation. Sci Rep 2016;6:39473.
25. Peng W, Chang M, Wu Y, et al. Lyophilized powder of mesenchymal stem cell supernatant attenuates acute lung injury through the IL-6-p-STAT3-p63-JAG2 pathway. Stem Cell Res Ther 2021;12:216.
26. Deng HF, Wang S, Wang XL, et al. Puerarin Protects Against LPS-Induced Vascular Endothelial Cell Hyperpermeability via Preventing Downregulation of Endothelial Cadherin. Inflammation 2019;42:1504-10.
27. Basit A, Reutershan J, Morris MA, et al. ICAM-1 and LFA-1 play critical roles in LPS-induced neutrophil recruitment into the alveolar space. Am J Physiol Lung Cell Mol Physiol 2006;291:L200-7.
28. Ulbrich H, Eriksson EE, Lindbom L. Leukocyte and endothelial cell adhesion molecules as targets for therapeutic interventions in inflammatory disease. Trends Pharmacol Sci 2003;24:640-7.
29. Lei J, Wei Y, Song P, et al. Cordycepin inhibits LPS-induced acute lung injury by inhibiting inflammation and oxidative stress. Eur J Pharmacol 2018;818:110-4.
30. Lee YM, Hybertson BM, Cho HG, et al. Platelet-activating factor contributes to acute lung leak in rats given interleukin-1 intratracheally. Am J Physiol Lung Cell Mol Physiol 2000;279:L75-80.
31. Tong W, Chen X, Song X, et al. Resveratrol inhibits LPS-

 

induced inflammation through suppressing the signaling cascades of TLR4-NF-κB/MAPKs/IRF3. Exp Ther Med 2020;19:1824-34.
32. Scozzi D, Liao F, Krupnick AS, et al. The role of neutrophil extracellular traps in acute lung injury. Front Immunol 2022;13:953195.
33. Zou P, Yang F, Ding Y, et al. Lipopolysaccharide downregulates the expression of ZO-1 protein through the Akt pathway. BMC Infect Dis 2022;22:774.
34. Mehta D, Malik AB. Signaling mechanisms regulating endothelial permeability. Physiol Rev 2006;86:279-367.
35. Dong W, He B, Qian H, et al. RAB26-dependent autophagy protects adherens junctional integrity in acute lung injury. Autophagy 2018;14:1677-92.
36. Gong H, Rehman J, Tang H, et al. HIF2α signaling inhibits adherens junctional disruption in acute lung injury. J Clin Invest 2015;125:652-64.
37. Hao Y, Wang T, Hou Y, et al. Therapeutic potential of Lianhua Qingke in airway mucus hypersecretion of acute exacerbation of chronic obstructive pulmonary disease. Chin Med 2023;18:145.

**Cite this article as:** Ma Y, Hou Y, Han Y, Liu Y, Han N, Yin Y, Wang X, Jin P, He Z, Sun J, Hao Y, Guo J, Wang T, Feng W, Qi H, Jia Z. Ameliorating lipopolysaccharide induced acute lung injury with Lianhua Qingke: focus on pulmonary endothelial barrier protection. J Thorac Dis 2024;16(10):6899-6917. doi: 10.21037/jtd-24-700